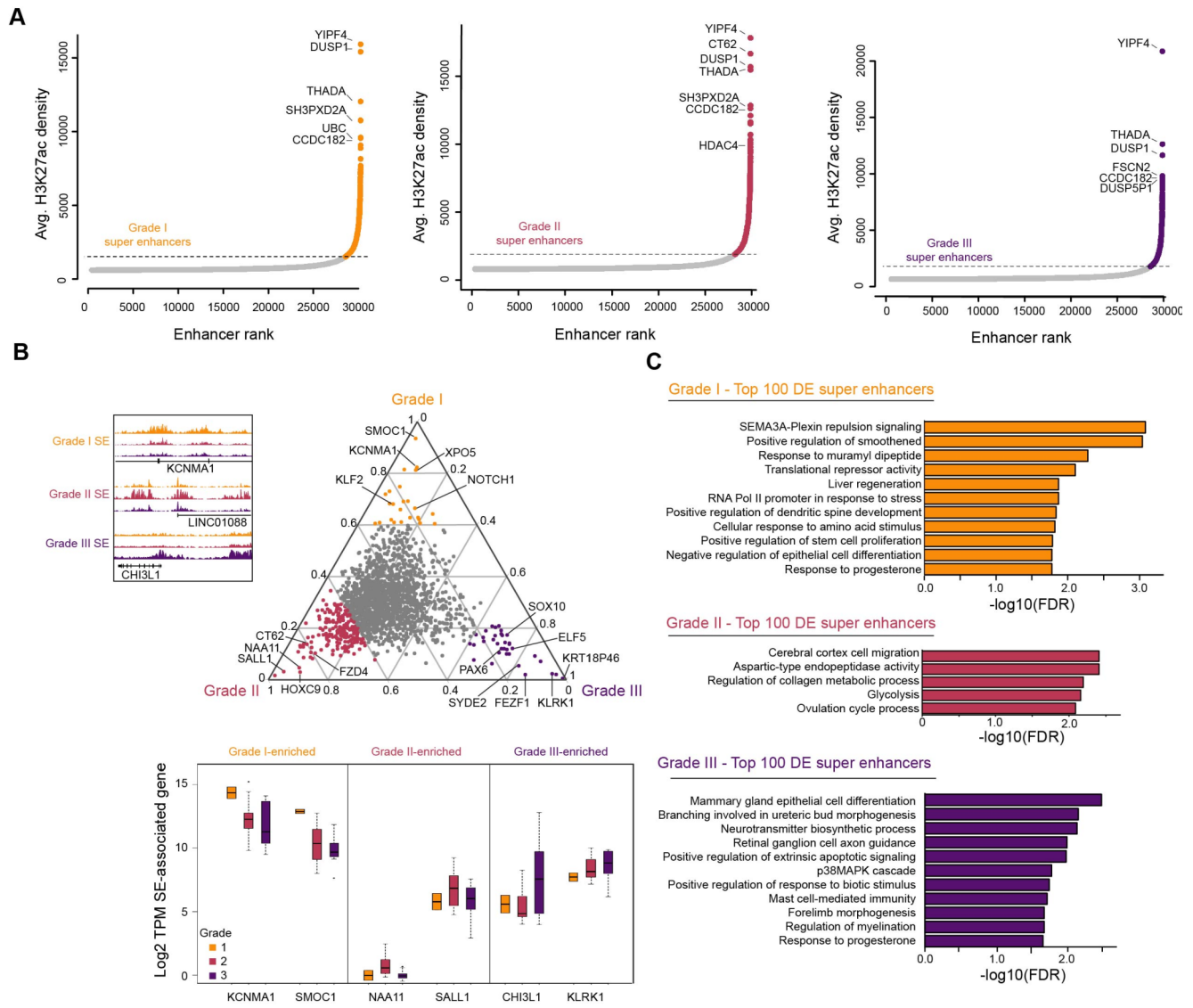
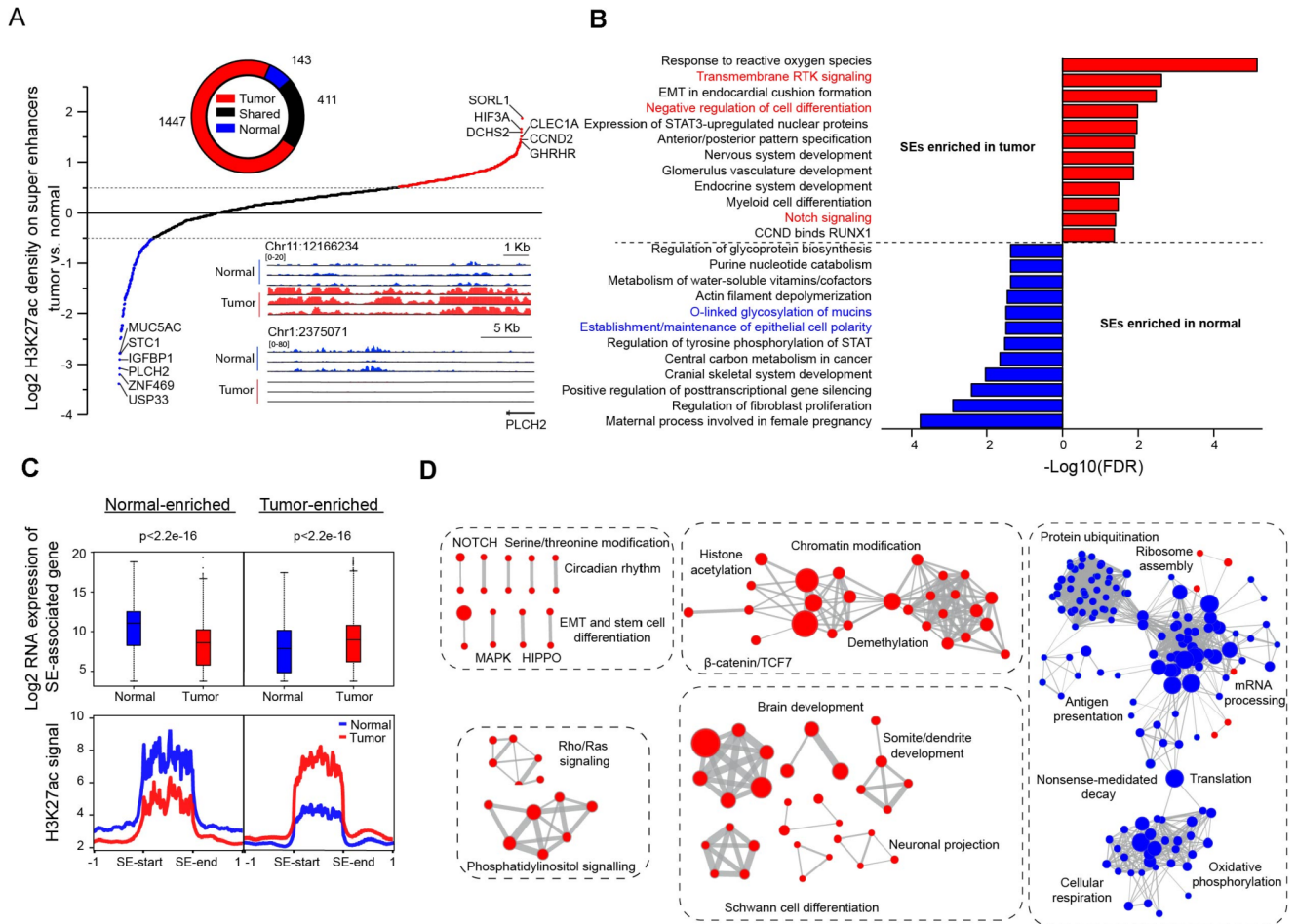


Supplementary Figure S2. H3K27ac clustering of meningiomas with tumor or normal tissue. (A) Consensus clustering of TCGA eRNA (left) and ENCODE Roadmap H3K27ac (right). K=5 was selected for each dataset based upon the peak in change in cumulative density function area. Top: Unsupervised hierarchical clustering at K=5 using Euclidean distance with dark blue indicating high correlation. **(B)** Unsupervised hierarchical clustering of Z-scores for enhancer cluster signal generated from the grade-of-membership model for ENCODE Roadmap H3K27ac was clustered into 5 groups, which were used to generate a grade of membership model. Tissue types were then clustered based upon signal from each group.



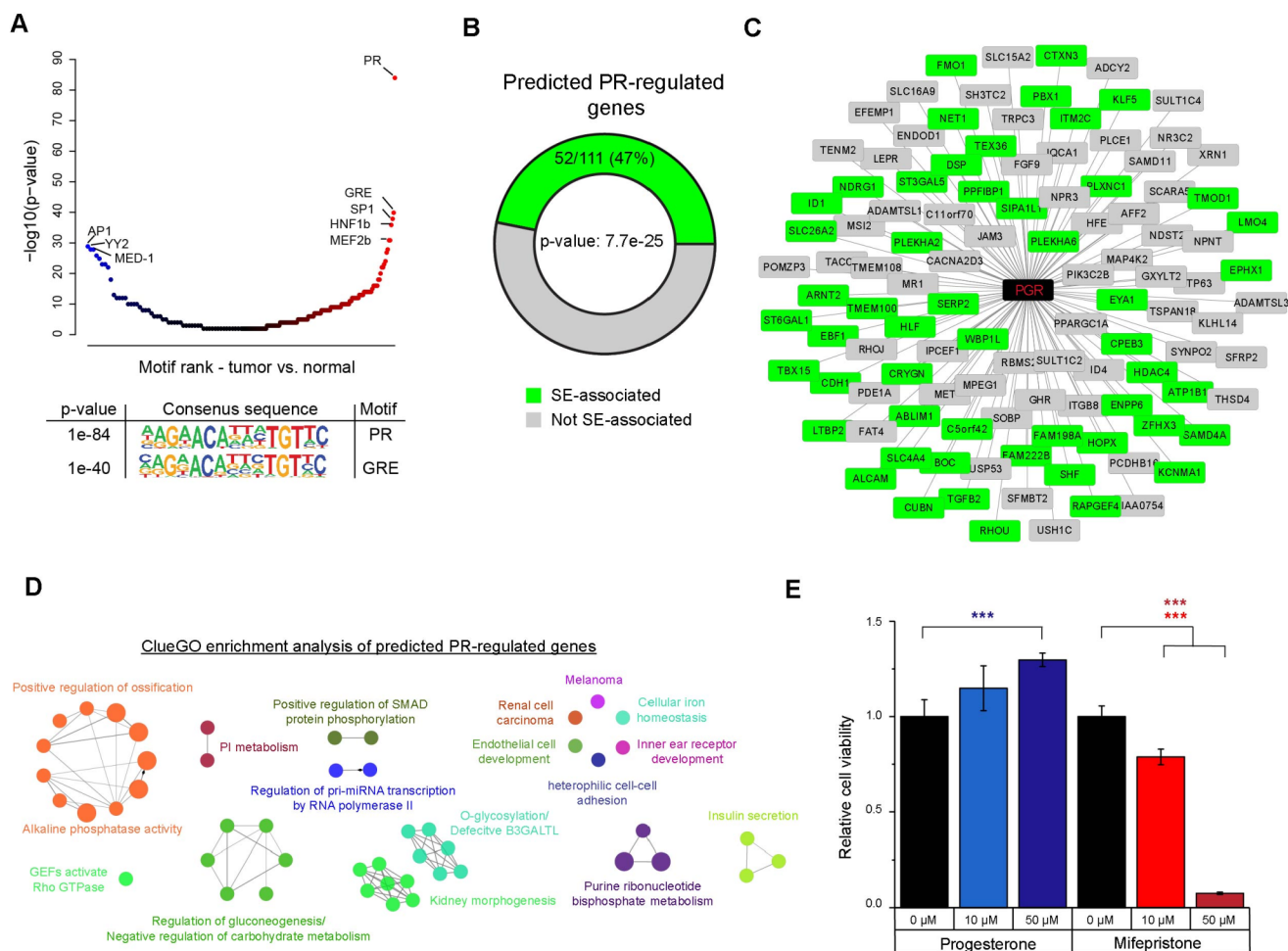
Supplementary Figure S3. Comparison of super enhancers across meningioma grades. (A) Plot of consensus super enhancers for each grade. Super enhancers (SEs) are defined as all enhancers above the inflection point of the graph. **(B)** Ternary plot of differential SEs between grades. For each SE the fold change per subgroup vs. overall average was calculated and transformed such that sum of squared fold changes for each SE equals 1. Colored points represent SEs that are enriched in a given grade for a value of >0.6 for that grade. Boxplots are represented as the median plus interquartile range. **(C)** ClueGO gene set enrichment analysis for grade-enriched SE-associated genes. Enrichment for GO BP, KEGG or Reactome pathways of the top 100 differentially enriched (DE) SE-associated genes for each grade.



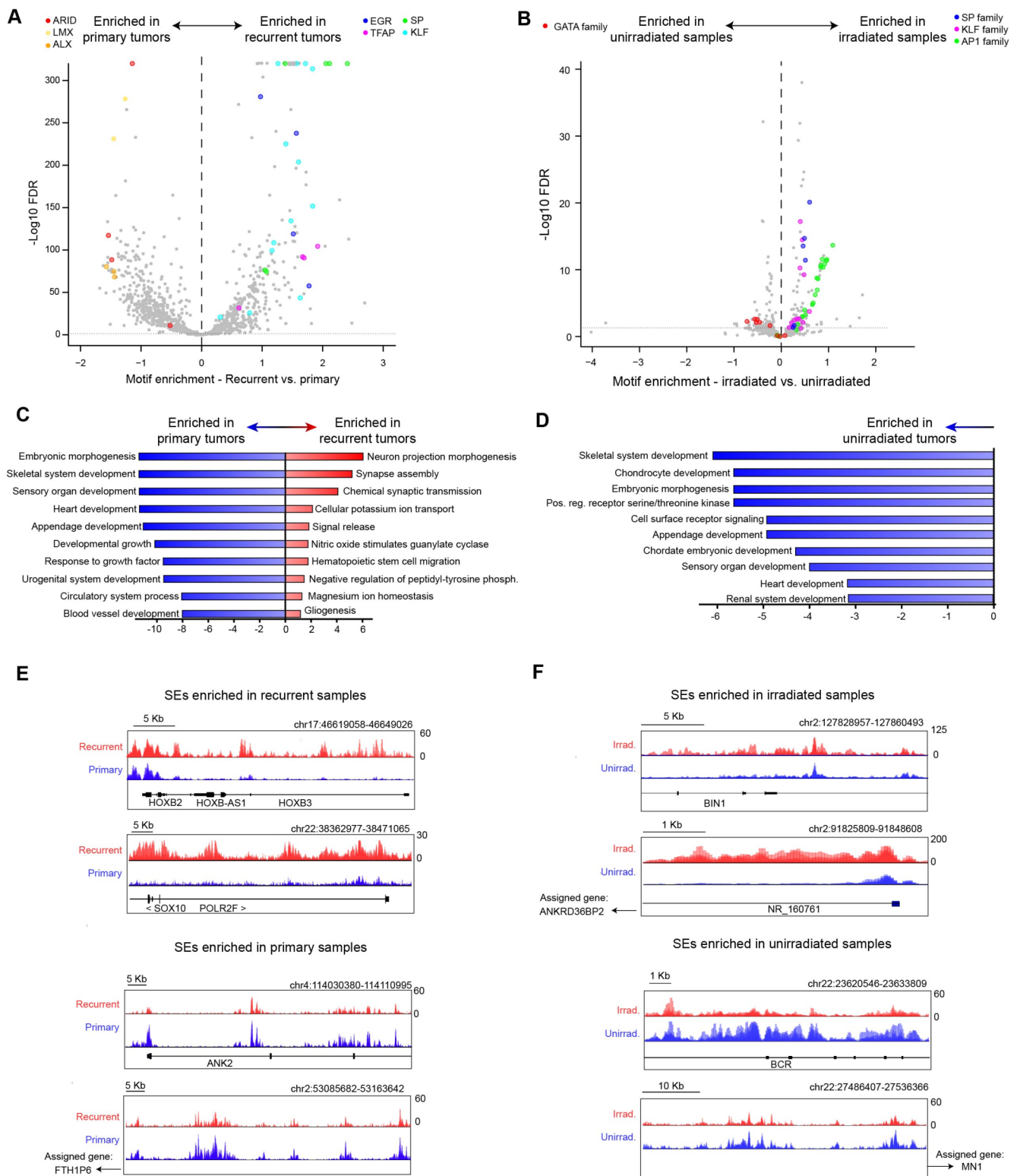
Supplementary Figure S4. Meningioma-specific enhancer signals segregate tumor vs. normal

samples. (A) Waterfall plot of tumor vs. normal fold change for each super enhancer (SE) ranked from negative enrichment (more signal in normal arachnoid granulation [AG]) to positive enrichment (more signal in tumor). Two representative tracks of differentially enriched SEs are below. The top track represents a tumor-enriched SE distally associated with SORL1 and the bottom one represents a normal AG-enriched SE associated with PLCH2. (B) Gene set enrichment analysis for genes associated with tumor-enriched SEs (red) or normal-enriched SEs (blue). Data are represented as mean \pm SD. (C) Summary statistics for differentially enriched SEs. Top: Genes associated with normal-enriched SEs are overexpressed at the transcriptional level in normal vs. tumor samples, while genes regulated by tumor-enriched SEs are overexpressed in tumors samples. Bottom: Trace of H3K27ac signal for tumor- or normal-enriched SEs. The red trace represents average signal from tumors. Blue represents the normal signal. Signal across normal-enriched SEs is on the left and

tumor-enriched SEs on the right. Boxplots are represented as the median plus interquartile range. **(D)** Gene set enrichment analysis for differentially expressed genes with a cutoff of $FDR < 0.05$ for a gene set. Edge weight is proportional to gene overlap and bubble size is proportional to significance of the gene set. Pathways are grouped based upon common function.



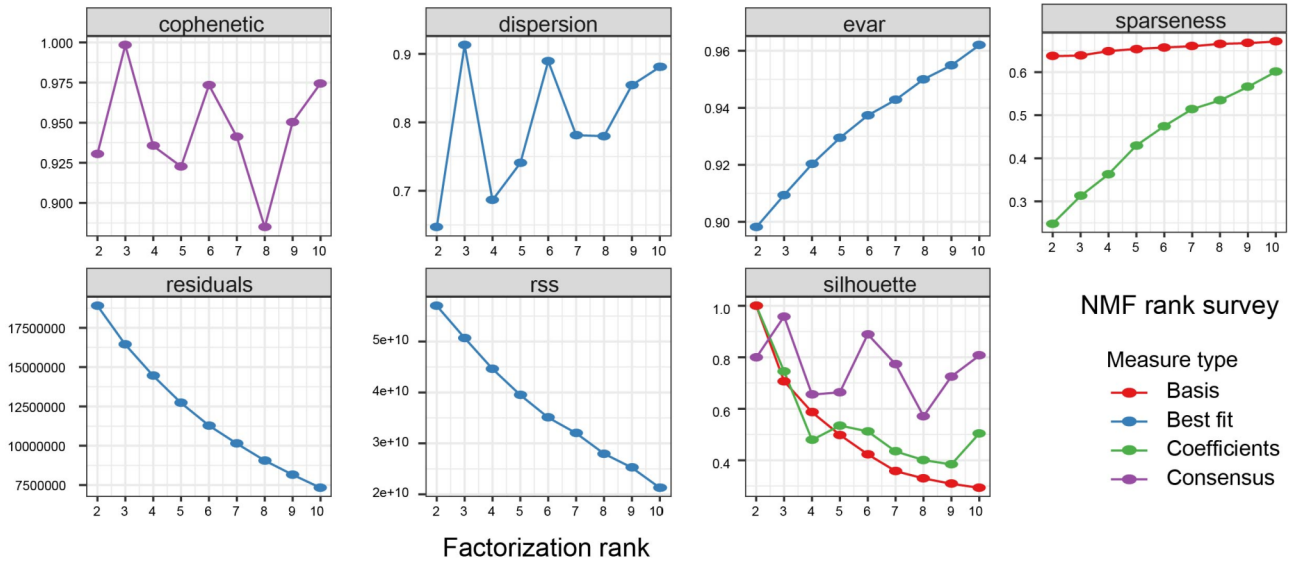
Supplementary Figure S5. Progesterone receptor in meningioma. (A) Differential motif enrichment in enhancers for tumor vs. normal samples. Motifs are ordered from most enriched in normal to most enriched in tumor. Consensus motifs are shown below for the top 2 most enriched tumor motifs. **(B)** Proportion of progesterone receptor-regulated genes that are SE-associated. Hypergeometric test p-value=7.7e-25. **(C)** Inferred progesterone receptor (PR) regulatory network. Genes in green are super-enhancer associated. **(D)** ClueGO gene set enrichment for PR signature genes using KEGG, Reactome and GO BP pathways at a cutoff of p<0.05. **(E)** Treatment of normal AG cells with progesterone or mifepristone. ANOVA followed by Tukey's HSD test was performed for all comparisons. ***, p-value<0.005.



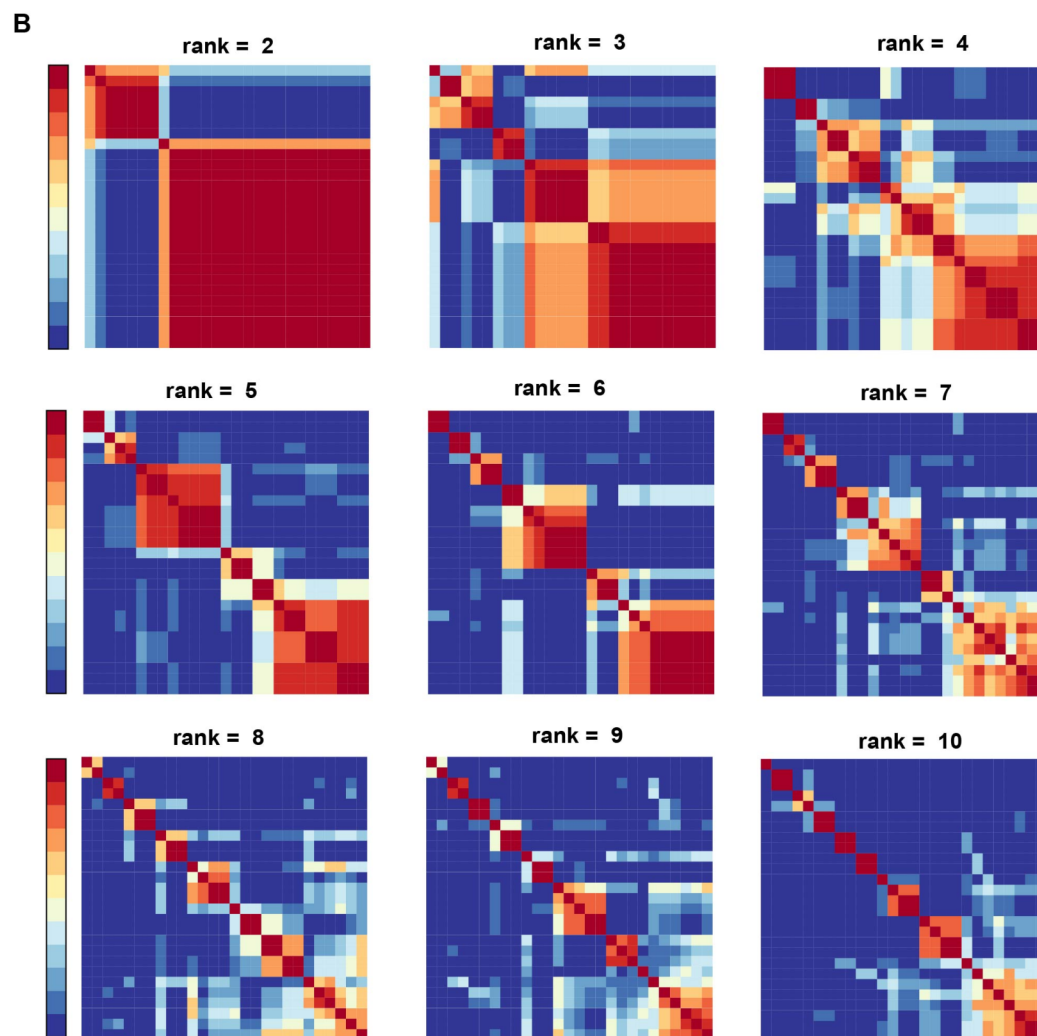
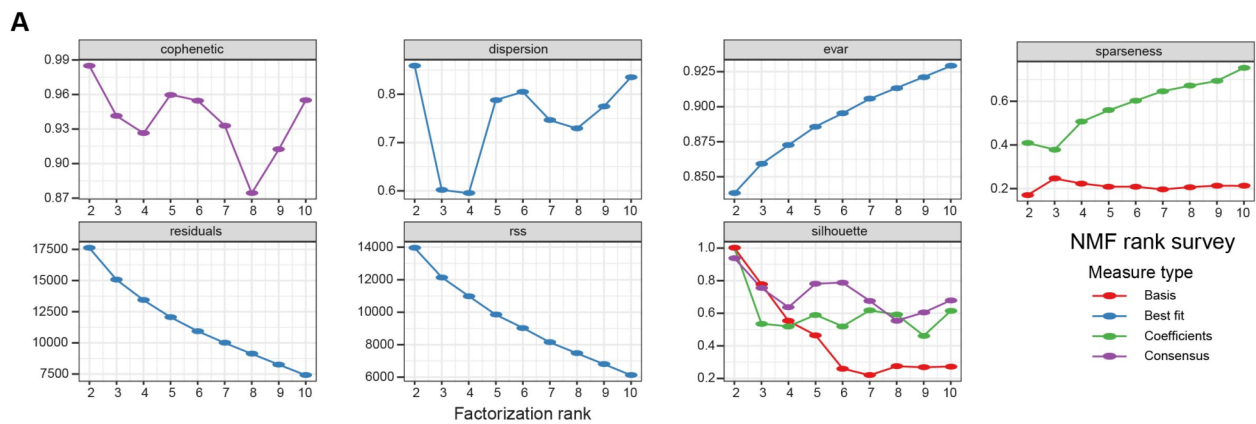
Supplementary Figure S6 . Enhancer and motif enrichments in irradiated or recurrent samples.

(A-B) Motifs enriched in the upregulated enhancers (p -value <0.05 , \log_2 fold change >1) in recurrent vs. primary **(A)** or irradiated vs unirradiated **(B)** tumors plotted as $-\log_{10}$ FDR on the y-axis vs. fold

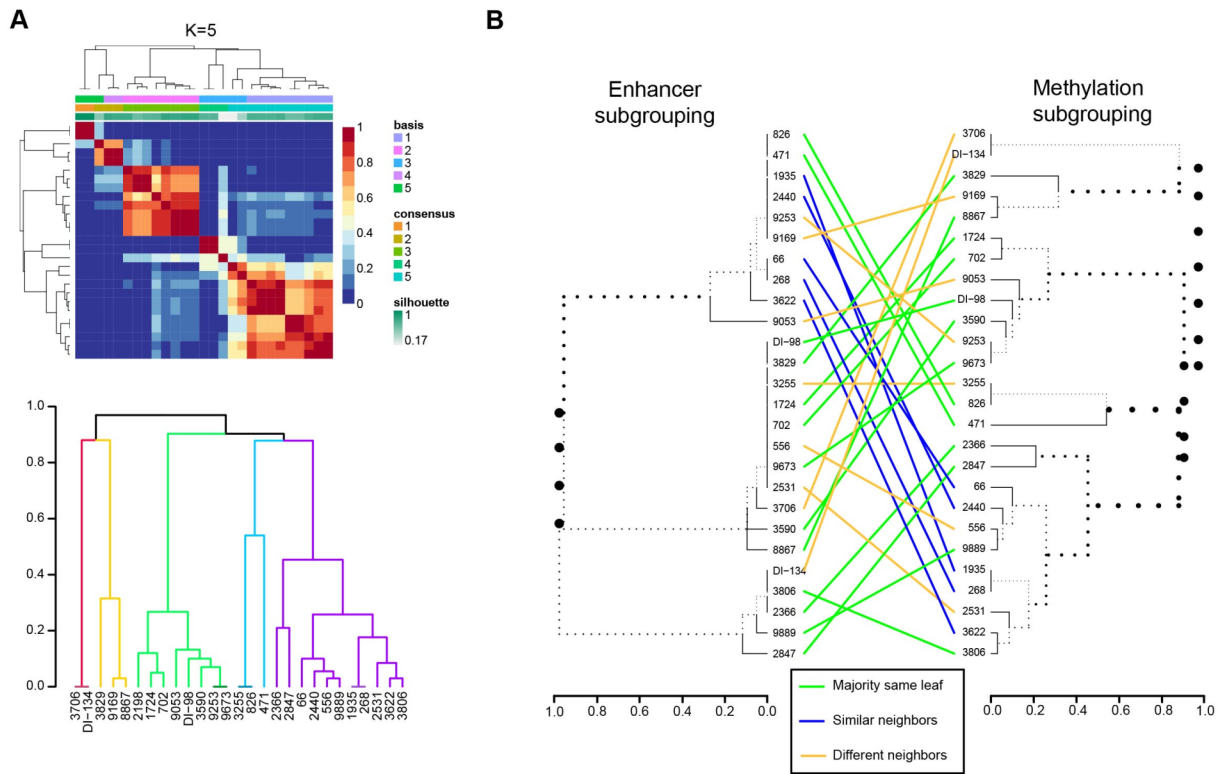
change of motif enrichment on the x-axis. Selected transcription factor families prevalent in one condition are called out in color. FDR values were derived using a Fisher exact test followed by Benjamini-Hochberg correction. **(C-D)** Gene set enrichment analysis of genes associated with enhancers differential (p-value 0.05 and log2 fold change >1) between recurrent (red) vs. primary (blue) **(C)** or irradiated (red) vs unirradiated (blue) **(D)** tumors. The $-\log_{10}$ FDR of the enrichment statistic is plotted on the y-axis. No pathways were significantly enriched in irradiated samples, although several were depleted. **(E-F)** Overlay of H3K27ac density for selected super enhancers enriched in recurrent **(E, top)**, primary **(E, bottom)**, irradiated **(F, top)** or unirradiated **(F, bottom)** samples.



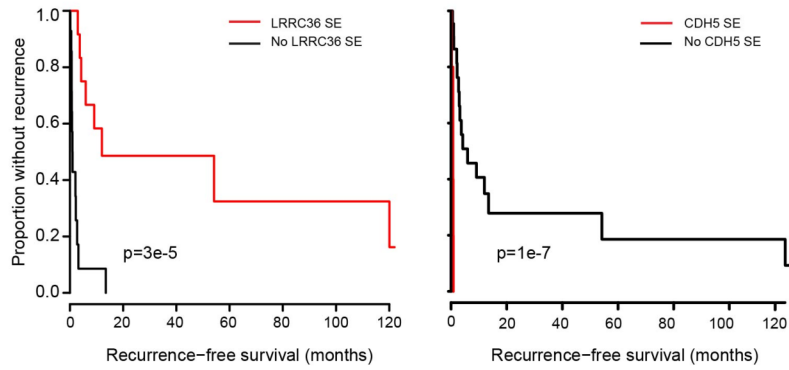
Supplementary Figure S7. NMF clustering of meningioma enhancers (A) Non-negative matrix factorization clustering metrics from K=2 to K=10 demonstrates optimal clustering at K=3.



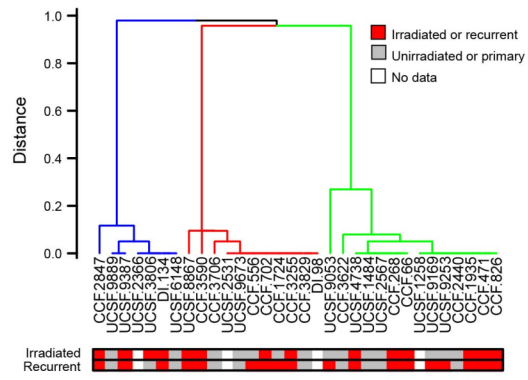
Supplementary Figure S8. NMF clustering of 450K methylation probes. (A) Clustering metrics for NMF clustering performed on the top 10% most variable probes from $K=2$ to $K=10$. **(B)** Corresponding consensus clustering maps for $K=2$ to $K=10$.



Supplementary Figure S9. Comparison of methylation cluster assignment with enhancer subgroup. **(A)** K=5 was selected as the best performing subgroup value based upon NMF metrics. **(B)** Tanglegram comparing enhancer subgroup (left) to methylation subgroup (right). Samples which retained the majority of their neighbors on the same major leaf were connected by green lines, while those with a subset of similar neighbors were connected by blue lines and those that segregated distinctly were annotated with an orange line.

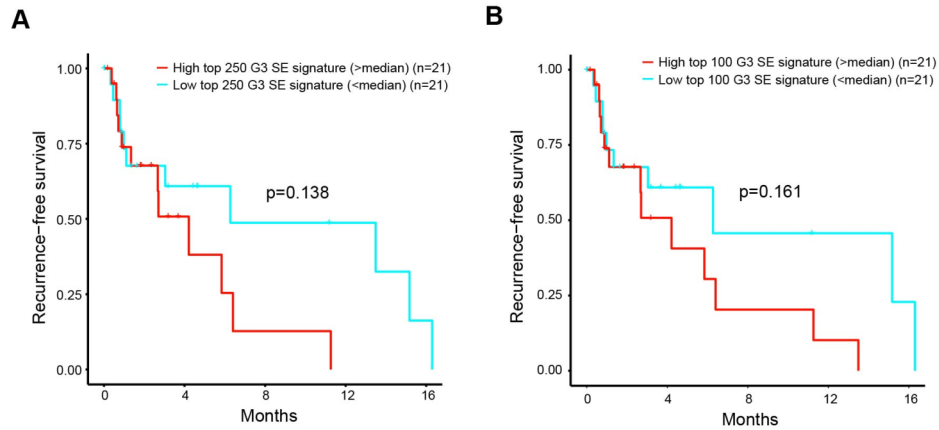


Supplementary Figure S10. Prognostic super enhancers. Kaplan-Meier plots of recurrence-free survival stratified by super enhancers (SEs) with prognostic significance based on logrank test.

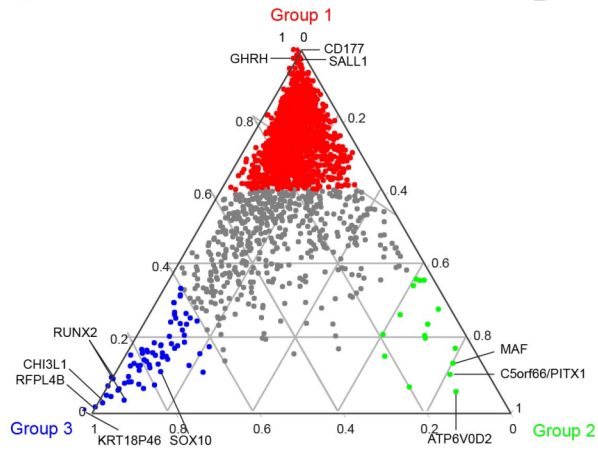
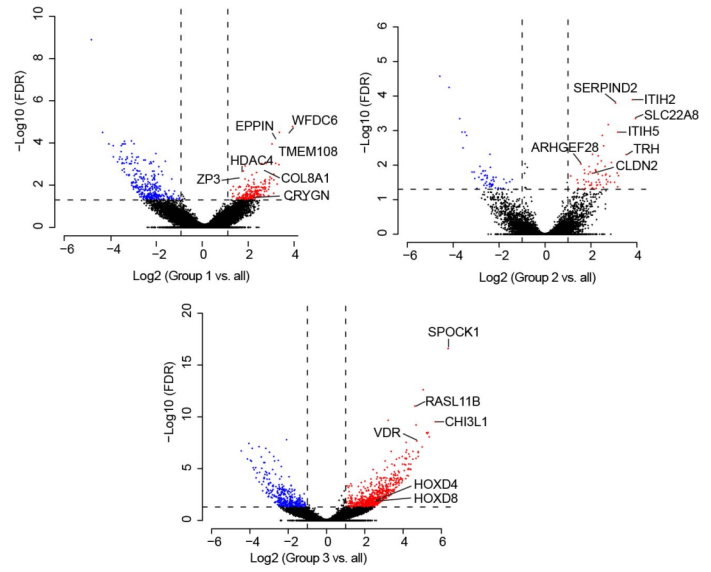
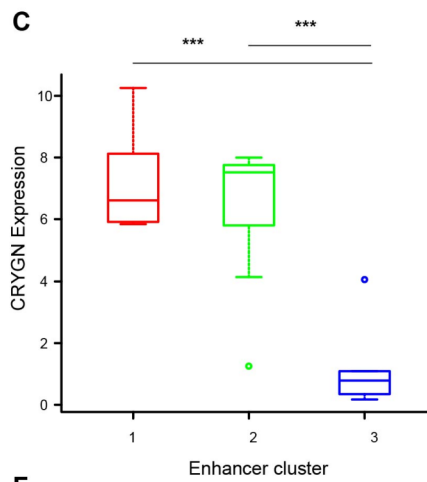
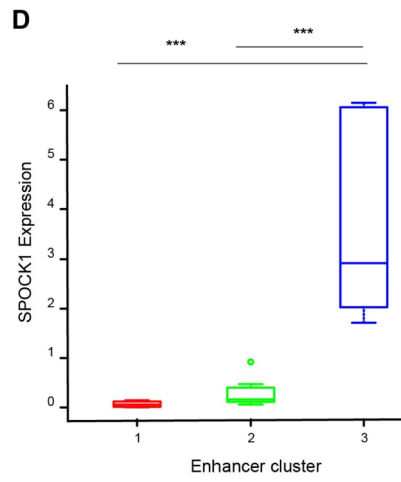
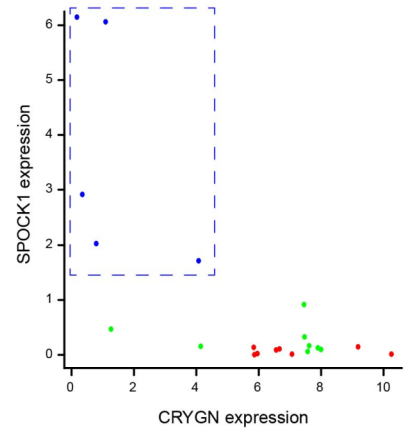
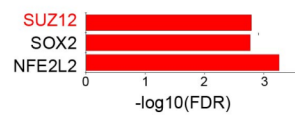
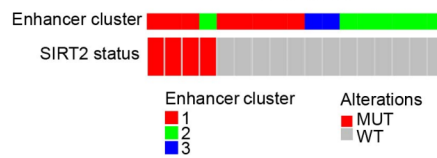
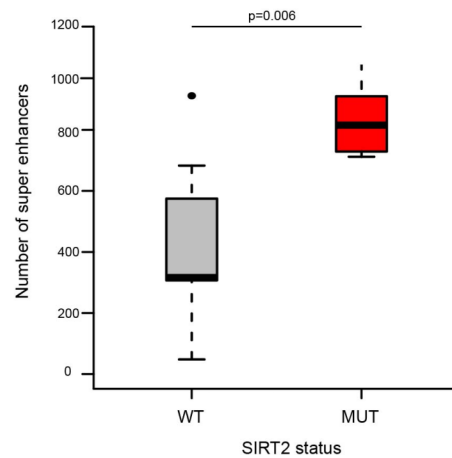


Supplementary Figure S11. Enhancer subgroup annotation by radiation or recurrence status.

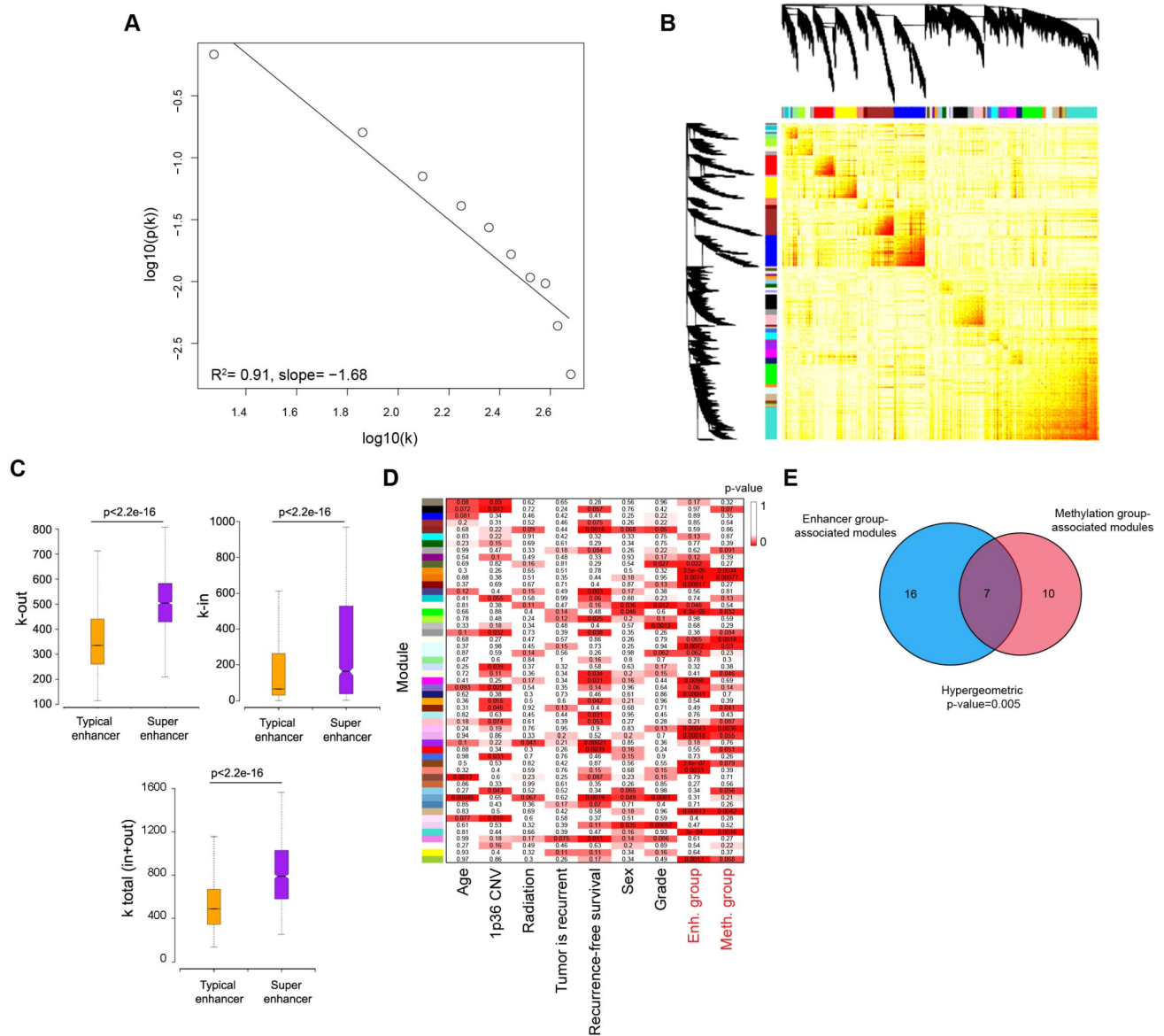
Enhancer clustering of meningiomas annotated by radiation or recurrence tumor status.



Supplementary Figure S12. Validation of an enhancer-derived prognostic signature in an independent cohort of meningioma biopsy specimens using gene expression. Single-sample gene set enrichment analysis was performed using the top 250 **(A)** or top 100 **(B)** super enhancer-associated genes. The cohort was then stratified at the median and p-values were derived using a logrank test.

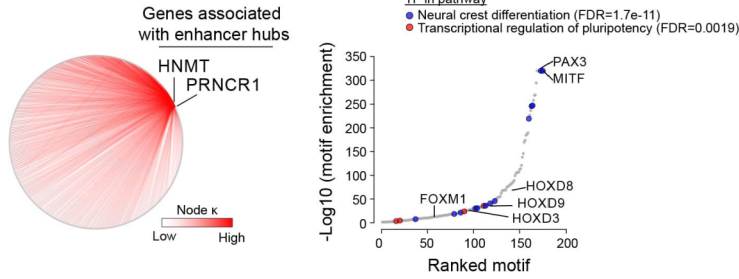
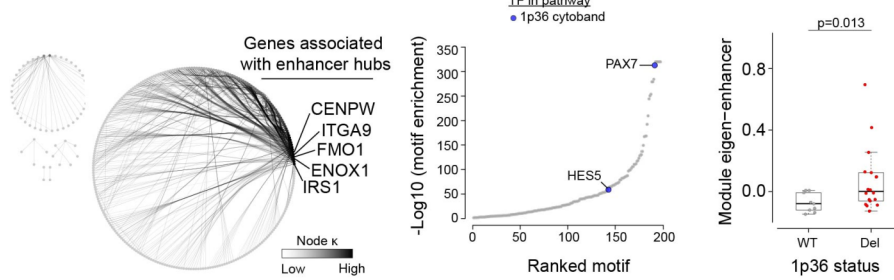
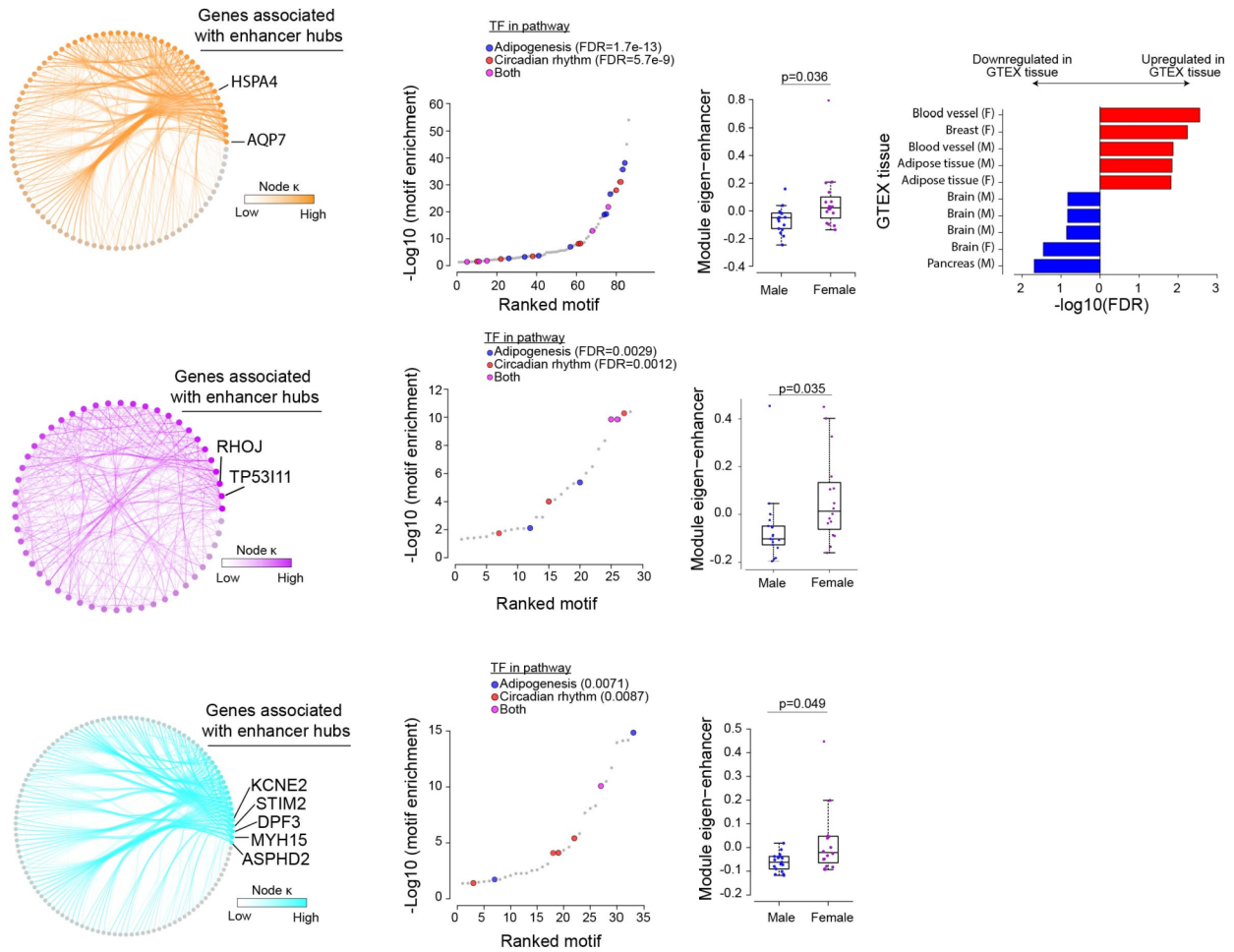
A**B****C****D****E****F****G**

Supplementary Figure S13. Comparison of meningioma subgroups. (A) Ternary plot of differential SEs between subgroups. For each SE the fold change per subgroup vs. overall average was calculated and transformed such that sum of squared fold changes for each SE equals 1. Colored points represent SEs that are enriched in a given subgroup for a value of >0.6 for that subgroup. **(B)** Volcano plots of RNA-seq comparing each subgroup with the rest of the cohort. Cutoffs for colored points are false discovery rate <0.05 and \log_2 fold change >1 or <-1 . **(C)** Expression of CRYGN, a top differentially expressed PR-regulated gene between subgroups 1 and 2 vs. 3. **(D)** Expression of SPOCK1, a top upregulated gene in subgroup 3 vs. 1 and 2. **(E)** Scatter plot of SPOCK1 vs. CRYGN expression, which effectively stratifies subgroups 1 and 2 from subgroup 3. **(F)** ChEA and ENCODE enrichment analysis of genes associated with gained SEs in group 1 tumors. SE-associated genes were enriched for targets of the polycomb repressive complex, SUZ12. **(G)** Presence of predicted deleterious SIRT2 mutations in the cohort shows enrichment in group 1 tumors. Super enhancer number in wildtype vs. mutant tumors was compared by student's t-test. SIRT2 mutations are associated with increased number of SEs. Boxplots are represented as the median plus interquartile range. *** $p<0.001$

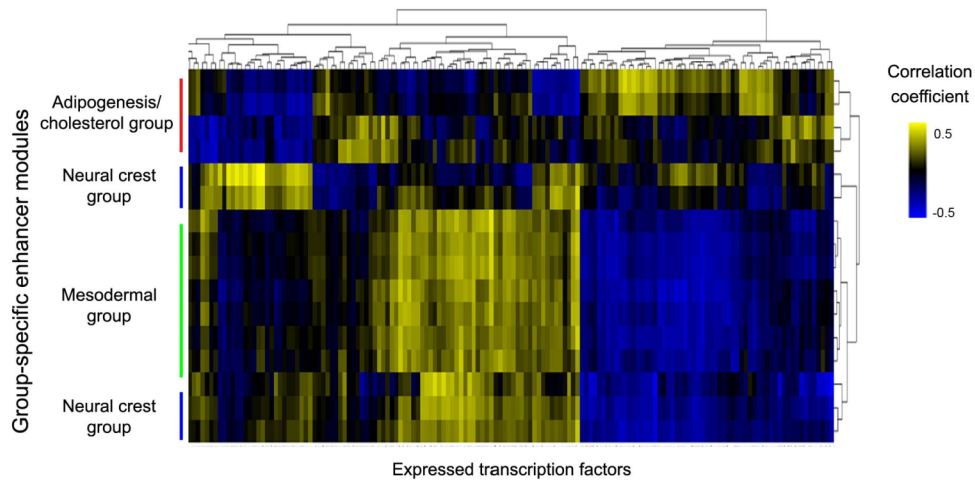


Supplementary Figure S14. Meningioma enhancer networks. (A) Weighted enhancer network demonstrates scale free topology. There are a small number of nodes, $p(k)$, that have a large number of connections (k), while the majority of nodes have a small number of connections. **(B)** Topological overlay matrix of enhancer signal. Module membership and dendrogram are indicated by the row and column annotation. Enhancers within the same module have higher overlap, indicated by darker color. **(C)** Boxplots comparing in-degree, out-degree and in+out-degree of typical enhancers vs super enhancers. Data were compared by student's t-test. Boxplots are represented as the median plus interquartile range. **(D)** Heatmap of the significance of association between module enhancers

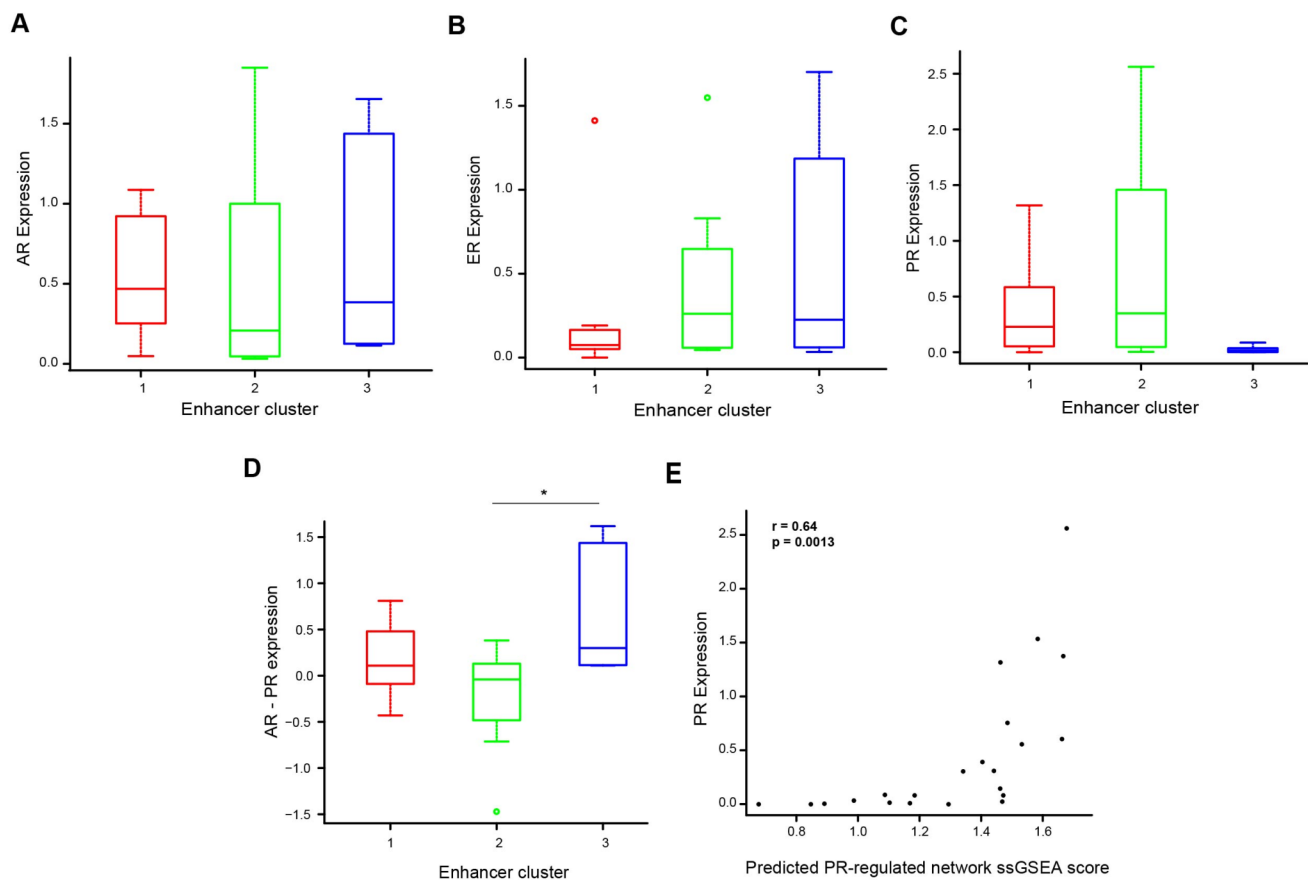
and clinical, epigenetic or genomic characteristics. For categorical variables, ANOVA test comparing groups was performed, for continuous variables, the significance of the Pearson correlation was reported. Student's t-test was used to compare between two groups. **(E)** Venn diagram of overlap between methylation-differential modules and enhancer subgroup-differential modules. Hypergeometric test was used to analyze overlap.

A**Recurrence-associated module****B****1p36-differential module****C****Sex-differential modules**

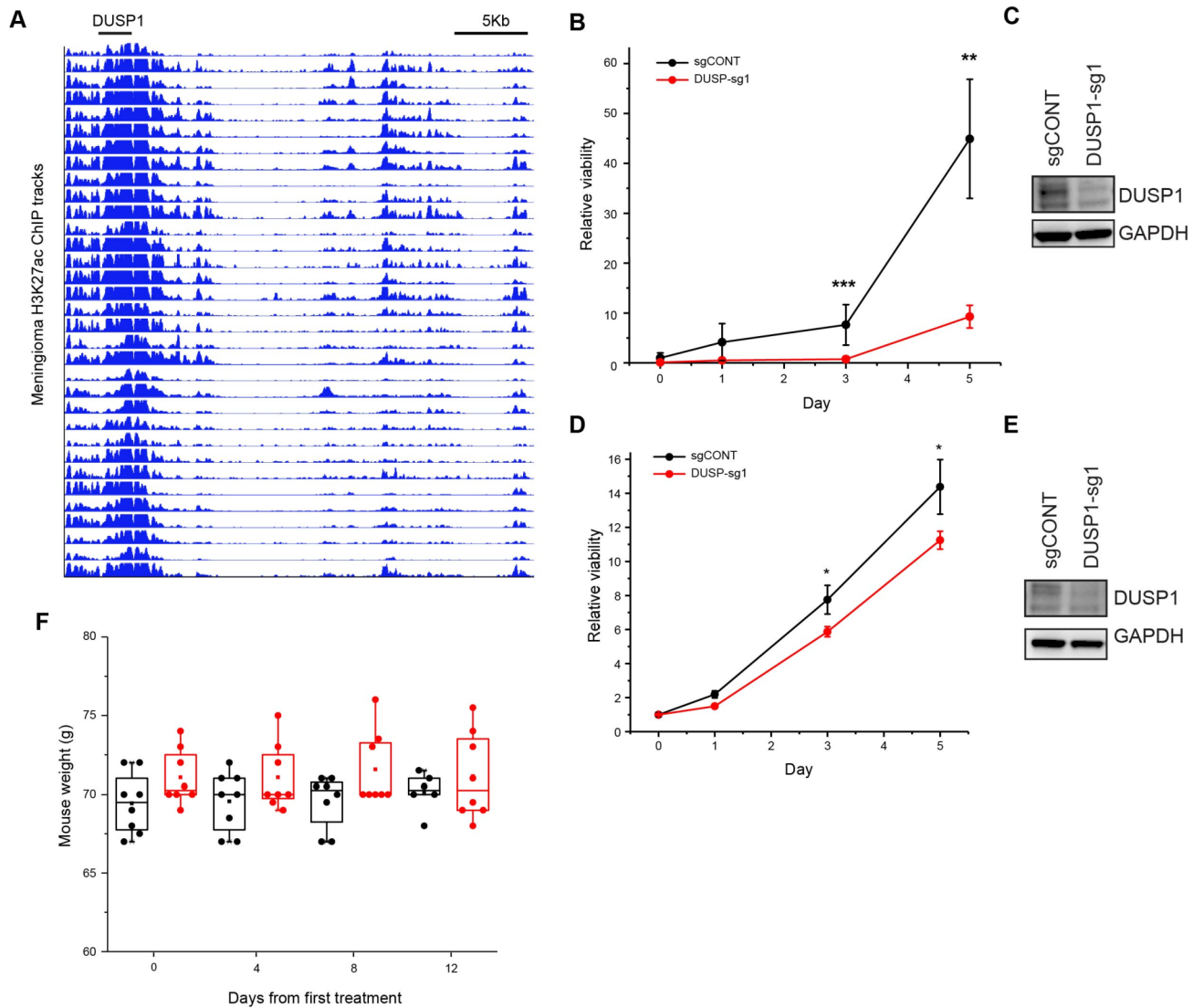
Supplementary Figure S15. Clinically correlated enhancer modules. (A) Module associated with rapid recurrence by Cox proportional hazards analysis using the module eigen-enhancer. Left: Module with top hubs annotated with enhancer-associated gene. Nodes are colored from grey to module color by node degree. Edges are drawn between nodes with a correlation coefficient of >0.4 . Right: transcription factors (TFs) ranked by motif enrichment in module vs. all enhancers. TFs in blue are annotated in the neural crest differentiation pathway. TFs in red are annotated in the transcriptional regulation of pluripotency. **(B)** Module enriched in 1p36-deleted tumors. Left: module plotted as above. Middle: TFs ranked by motif enrichment in module vs. all enhancers. TFs in blue are found on 1p36. Right: boxplot of module eigen-enhancer by 1p36 status, compared using student's t-test. **(C)** Sex-differential modules. Left: Modules plotted as above. Middle-left: TFs ranked by motif enrichment in module vs. all enhancers. TFs in blue are annotated in adipogenesis. TFs in red are annotated in circadian rhythm regulation. Middle-right: boxplot of module eigen-enhancer by patient sex, compared using student's t-test. Top-Right: TFs enriched in this module are also enriched in genotype-tissue expression project (GTEx) adipose and breast tissue and downregulated in GTEx brain tissue. Boxplots are represented as the median plus interquartile range.



Supplementary Figure S16. Heatmap of correlation between transcription factor expression and module eigen-enhancer for subgroup-enriched modules. Rows are eigen-enhancers for each module that is differentially enriched between subgroups (ANOVA p -value <0.1). Columns are normalized transcription factor expression from RNA-seq data. Pearson correlation coefficients were calculated between each transcription factor and eigen-enhancer. Subgroup specific modules are indicated by red, blue or green bars to the right of the plot. Unsupervised hierarchical clustering by Euclidean distance re-stratified subgroups as indicated by the clustering of subgroup-enriched modules.



Supplementary Figure S17. Correlation of enhancer subgroup with clinically implementable markers expression. (A-C) Transcript expression of androgen receptor (AR) **(A)**, estrogen receptor (ER) **(B)** and progesterone receptor (PR) **(C)** across subgroups. Log2 TPM values are plotted on the y-axis. **(D)** Differential expression of AR vs. PR by subgroup. **(E)** Correlation between PR and PR-regulated network signature.



Supplementary Figure S18. DUSP1 is a meningioma dependency. (A) H3K27ac signal at the DUSP1 super enhancer. **(B)** Relative cell viability following CRISPR-Cas9 DUSP1 knockout in CH157-MN compared to non-targeting control. **(C)** Western blot demonstrating DUSP1 knockout efficiency in CH157-MN. **(D)** Relative cell viability following CRISPR-Cas9 DUSP1 knockout in IOMM-Lee compared to non-targeting control. **(E)** Western blot demonstrating DUSP1 knockout efficiency in IOMM-Lee. P-values were calculated using Student's t-test. **(F)** Mouse weight in grams plotted by day after the beginning of BCI treatment. Boxplots are represented as the median plus interquartile range. * $p < 0.05$, ** $p < 0.005$, *** $p < 0.0005$

| Variable | | Value |
|---------------------------------------|----------------------|------------------|
| Grade | | |
| | I | 9 (27%) |
| | II | 11 (33%) |
| | III | 12 (36%) |
| Male | | 16 (48%) |
| Age | | 58.9 [52.0-65.8] |
| Hx/o radiation | | 14 (42%) |
| Recurrent | | 18 (54%) |
| RFS | | 17.3 [0.3-34.3] |
| Died | | 8 (24%) |
| OS | | 35.3 [15.8-54.7] |
| GTR | | 16 (48%) |
| Location | | |
| | Frontal | 7 (21%) |
| | Parasagittal | 5 (15%) |
| | Tentorial | 2 (6%) |
| | Parietal | 1 (3%) |
| | Temporal | 1 (3%) |
| | Sphenoid | 3 (9%) |
| | Skull base | 2 (6%) |
| | Cavernous | 1(3%) |
| | Clinoidal | 1 (3%) |
| | Occipital | 2 (6%) |
| | Olfactory | 1 (3%) |
| Bone invasion | | 10 (30%) |
| Brain invasion | | 12 (36%) |
| NF2 loss | | 22 (67%) |
| 1p36 loss | | 18 (55%) |
| Heidelberg methylation cluster | | |
| | Benign | 3 (9%) |
| | Intermediate | 13 (39%) |
| | Malignant | 7 (21%) |
| | Not classified/other | 3 (9%) |
| Enhancer cluster | | |
| | 1 | 11 (33%) |
| | 2 | 7 (21%) |
| | 3 | 14 (42%) |
| | NA | 1 (3%) |

Supplementary Table 1. Cohort characteristics. Data represented as number (% of total) or mean [95% confidence interval]. RFS: recurrence-free survival; OS: overall survival; GTR: gross-total resection

| Variable | | Hazard ratio [95% CI] | p-value |
|-------------------------------------|--------------|-----------------------|--------------|
| Grade | | | 0.25 |
| | II | 1.82 [0.60-5.53] | 0.29 |
| | III | 2.44 [0.83-7.19] | 0.11 |
| Sex | Female | 0.55 [0.23-1.31] | 0.17 |
| Age | | 1.01 [0.98-1.03] | 0.67 |
| Hx/o radiation | | 3.07 [1.16-8.13] | 0.02 |
| Recurrent | | 1.54 [0.59-4.02] | 0.37 |
| GTR | | 0.38 [0.16-0.92] | 0.03 |
| Invasion | | 1.65 [0.66-4.15] | 0.17 |
| NF2 status | | 0.53 [0.17-1.69] | 0.28 |
| 1p36 status | | 1.02 [0.37-2.83] | 0.97 |
| Heidelberg methylation cluster | | | 0.88 |
| | Intermediate | 1.97 [0.37-10.39] | 0.42 |
| | Malignant | 1.80 [0.31-10.48] | 0.51 |
| | Unclassified | 1.59 [0.22-11.58] | 0.65 |
| Cohort-specific methylation cluster | | | 0.14 |
| | Group 2 | 6.34 [1.03-38.96] | 0.046 |
| | Group 3 | 1.51 [0.49-4.67] | 0.478 |
| | Group 4 | 0.89 [0.20-3.99] | 0.88 |
| | Group 5 | 0.63 [0.22-1.84] | 0.40 |
| Enhancer cluster | | | 0.02 |
| | Group 2 | 0.95 [0.33-2.78] | 0.93 |
| | Group 3 | 3.80 [1.17-12.28] | 0.03 |

Supplementary Table 2. Univariable analysis of factors associated with recurrence-free survival. Bold: p<0.1. GTR: gross-total resection; CI: confidence interval

| Variable | Hazard ratio [95% CI] | p-value |
|------------------|------------------------------|----------------|
| Hx/o radiation | 5.97 [1.79-19.92] | 0.004 |
| GTR | 0.46 [0.18-1.19] | 0.11 |
| Enhancer cluster | | 0.052 |
| Group 2 | 1.35 [0.45-4.08] | 0.59 |
| Group 3 | 6.41 [1.65-24.92] | 0.0074 |

Supplementary Table 3. Multivariable analysis of factors associated with recurrence-free survival. Bold: p<0.1. GTR: gross-total resection; CI: confidence interval

| Super enhancer coordinates | Associated gene | Hazard ratio | 5% | 95% | FDR |
|----------------------------|-----------------|--------------|-----|-------|--------|
| chr16:66274800-66307968 | CDH5 | 41.9 | 4.6 | 378.5 | 0.0002 |
| chr17:3401687-3440786 | OR1AC1P | 15.1 | 3 | 77.2 | 0.0049 |
| chr5:34486801-34536263 | BRIX1 | 15.1 | 3 | 77.2 | 0.0049 |
| chr7:46780071-46813699 | AC011294.3 | 15.1 | 3 | 77.2 | 0.0049 |
| chr2:174847219-174928725 | HNRNPA1P39 | 12.6 | 3 | 52.8 | 0.0049 |
| chr2:175189736-175209834 | AC018470.1 | 11.4 | 2.2 | 59.1 | 0.032 |
| chr7:129989908-130040817 | COPG2 | 11.4 | 2.2 | 59.1 | 0.032 |
| chr9:98788402-98846818 | EIF4BP3 | 11.4 | 2.2 | 59.1 | 0.032 |
| chr17:73965997-74001021 | PRCD | 10.5 | 2.4 | 44.8 | 0.0186 |
| chr6:151308505-151424271 | MTHFD1L | 9.5 | 2.2 | 40.7 | 0.032 |
| chr6:74224148-74234180 | RPS27P15 | 8.7 | 2 | 37 | 0.0462 |
| chr7:25642672-25772070 | C7orf31 | 8.7 | 2.1 | 36.7 | 0.046 |
| chr19:17178164-17265385 | MYO9B | 7.9 | 1.9 | 33.7 | 0.067 |
| chr6:163816942-163850017 | AL078585.1 | 7.9 | 1.9 | 33.7 | 0.067 |
| chr13:110869743-111074938 | COL4A2 | 7.6 | 2.3 | 25.4 | 0.0211 |
| chr9:67288204-67303335 | FAM27B | 7.3 | 1.8 | 29.6 | 0.0786 |
| chr13:97862114-97933029 | MBNL2 | 7.2 | 1.7 | 30.6 | 0.0937 |
| chr9:139398087-139467250 | NOTCH1 | 6.6 | 1.9 | 23.2 | 0.0646 |
| chr8:49282938-49353609 | RPL29P19 | 6.2 | 1.8 | 21.6 | 0.0786 |
| chr20:23062605-23145984 | THBD | 6 | 1.9 | 19.5 | 0.0641 |
| chr14:55544354-55598892 | RP11-665C16.8 | 5.9 | 1.7 | 20.5 | 0.0836 |
| chr2:102307734-102467979 | AC092570.3 | 5.9 | 1.7 | 20.5 | 0.0836 |
| chr11:75012845-75064145 | ARRB1 | 5.8 | 1.8 | 18.3 | 0.067 |
| chr2:191461663-191529308 | MFSD6 | 5.6 | 1.7 | 18.5 | 0.0855 |
| chr16:67318101-67355058 | LRRC36 | 0.1 | 0 | 0.4 | 0.0064 |

Supplementary Table 4. Individual super enhancers with prognostic significance. Each super enhancer (SE) was tested for prognostic significance using the logrank test based on the presence vs. absence of the SE in the sample. P-values were adjusted to false discovery rate using Benjamini-Hochberg correction. FDR: false discovery rate

| Variable | Value |
|-------------------------|------------------|
| Grade | |
| I | 7 (50%) |
| II | 7 (50%) |
| III | - |
| Male | 3 (21%) |
| Age | 59.5 [53.0-66.0] |
| Hx/o radiation | 1 (7%) |
| Recurrent | 5 (36%) |
| RFS | 53.0 [26.0-80.0] |
| Died | 4 (29%) |
| OS | 62.2 [36.7-87.8] |
| GTR | 10 (71%) |
| Location | |
| Frontal | 4 (29%) |
| Parasagittal | 1 (7%) |
| Tentorial | 2 (14%) |
| Parietal | 1 (7%) |
| Temporal | 2 (14%) |
| Sphenoid | 2 (14%) |
| Skull base | 2 (14%) |
| Bone invasion | 1 (7%) |
| Brain invasion | 2 (14%) |
| Enhancer cluster | |
| 1 | 4 (29%) |
| 2 | 3 (21%) |
| 3 | 7 (50%) |

Supplementary Table 5. Clinical characteristics of the validation cohort. Data are represented as number (% of total) or mean [95% confidence interval]. RFS: recurrence-free survival; OS: overall survival; GTR: gross-total resection

| Variable | | Hazard ratio [95% CI] | p-value |
|------------------------|---------|------------------------------|----------------|
| Grade | II | 4.58 [0.50-41.7] | 0.12 |
| Sex | Female | 1.71 [0.19-15.45] | 0.65 |
| Age | | 0.98 [0.90-1.06] | 0.57 |
| Hx/o radiation* | | 11.49 [0.72-183.8] | 0.03 |
| Recurrent | | 1.52 [0.25-9.16] | 0.61 |
| GTR | | 2.42 [0.24-24.41] | 0.46 |
| Bone or brain invasion | | 0.59 [0.065-5.3] | 0.65 |
| Enhancer cluster | | | 0.22 |
| | Group 2 | 0.59 [0.065-5.3] | 0.63 |
| | Group 3 | 5.06 [0.53-48.45] | 0.12 |

Supplementary Table 6. Predictors of recurrence in the validation cohort. Bold: $p \leq 0.1$; *Only one sample. CI: confidence interval; GTR: gross-total resection

| Model | Sex | Age | NF2 status | Mutation | Grade | Enhancer cluster |
|-----------------|------------|------------|-------------------|-----------------|--------------|-------------------------|
| CH157-MN | F | 41 | Loss | NRAS | NA | NA |
| IOMM-Lee | M | 61 | Intact | BRAF | 3 | NA |
| DI-98 | M | NA | Loss | NA | 2 | 1 |
| DI-134 | F | NA | Loss | SUFU | 2 | 2 |
| 3810 | F | 61 | NA | NA | 1 | 1 |
| 3999 | F | 52 | NA | NA | 1 | NA |

Supplementary Table 7. Characteristics of models used for functional studies. NA, Not available.